

Extraordinary transmission through metal-coated monolayers of microspheres

L. Landström¹, D. Brodoceanu², D. Bäuerle², F. J. Garcia-Vidal³, Sergio G. Rodrigo, and L. Martin-Moreno⁴

¹The Ångström Laboratory, Department of Materials Chemistry, Uppsala University, Box 538, SE-751 21 Uppsala, Sweden
lars.landstrom@mkem.uu.se

²Institut für Angewandte Physik, Johannes-Kepler-Universität Linz, A-4040, Linz, Austria

³Departamento de Física Teórica de la Materia Condensada, Universidad Autónoma de Madrid, E-28049 Madrid, Spain

⁴Instituto de Ciencia de Materiales de Aragon and Dept. de Física de la Materia Condensada, CSIC-Universidad de Zaragoza, E-50015 Zaragoza, Spain

Abstract: The spectral dependence of the extraordinary transmission through monolayers of close-packed silica or polystyrene microspheres on a quartz support, covered with different thin metal films (Ag, Au and Ni) was investigated. The measured spectra were compared with modeled transmission spectra using finite difference time domain (FDTD) calculations. Measured and modeled spectra show good overall agreement. The supported modes in the sphere array were found to be of utmost importance for the transmission mechanism and the results also suggest that the presence of guided modes in the photonic crystal may further enhance the extraordinary transmission through the metal film.

© 2009 Optical Society of America

OCIS codes: (240.6680) Surface plasmons, (250.5403) Plasmonics, (350.4238) Nanophotonics and photonic crystals

References and links

1. W. L. Barnes, A. Dereux, and T. W. Ebbesen, "Surface plasmon subwavelength optics," *Nature* **424**, 824 (2003).
2. C. Genet and T. W. Ebbesen, "Light in tiny holes," *Nature* **445**, 39–46 (2007).
3. T. Ebbesen, H. Lezec, H. Ghaemi, T. Thio, and P. Wolff, "Extraordinary optical transmission through subwavelength hole arrays," *Nature* **391**, 667 (1998).
4. D. E. Grupp, H. J. Lezec, T. W. Ebbesen, K. M. Pellerin, and T. Thio, "Crucial role of metal surface in enhanced transmission through subwavelength apertures," *Appl. Phys. Lett.* **77**, 1569 (2000).
5. L. Martin-Moreno, F. J. Garcia-Vidal, H. J. Lezec, K. M. Pellerin, T. Thio, J. B. Pendry, and T. W. Ebbesen, "Theory of Extraordinary Optical Transmission through Subwavelength Hole Arrays," *Phys. Rev. Lett.* **86**, 1114 (2001).
6. Q. Wang, J. Li, C. Huang, C. Zhang, and Y. Zhu, "Enhanced optical transmission through metal films with rotation-symmetrical hole arrays," *Appl. Phys. Lett.* **87**, 091105 (2005).
7. J. R. Krenn *et al.*, "Squeezing the Optical Near-Field Zone by Plasmon Coupling of Metallic Nanoparticle," *Phys. Rev. Lett.* **82**, 2590 (1999).
8. H. J. Lezec, A. Degiron, E. Devaux, R. A. Linke, L. Martin-Moreno, F. J. Garcia-Vidal, and T. W. Ebbesen, "Beaming Light from a Subwavelength Aperture," *Science* **297**, 820 (2002).

9. D. E. Grupp, H. Lezec, T. Thio, and T. Ebbesen, "Beyond the Bethe Limit: Tunable Enhanced Light Transmission Through a Single Sub-Wavelength Aperture," *Adv. Mater.* **11**, 860 (1999).
10. Y.-H. Ye and J.-Y. Zhang, "Middle-infrared transmission enhancement through periodically perforated metal films," *Appl. Phys. Lett.* **84**, 2977 (2004).
11. K. L. van der Molen, F. B. Segerink, N. F. van Hulst, and L. Kuipers, "Influence of hole size on the extraordinary transmission through subwavelength hole arrays," *Appl. Phys. Lett.* **85**, 4316 (2004).
12. D. Qu and D. Grischkowsky, "Observation of a New Type of THz Resonance of Surface Plasmons Propagating on Metal-Film Hole Arrays," *Phys. Rev. Lett.* **93**, 196804 (2004).
13. C. Janke, J. G. Rivas, C. Schotsch, L. Beckmann, P. H. Bolivar, and H. Kurz, "Optimization of enhanced terahertz transmission through arrays of subwavelength apertures," *Phys. Rev. B* **69**, 205314 (2004).
14. W. L. Barnes, W. A. Murray, J. Dintinger, E. Devaux, and T. Ebbesen, "Surface Plasmon Polaritons and Their Role in the Enhanced Transmission of Light through Periodic Arrays of Subwavelength Holes in a Metal Film," *Phys. Rev. Lett.* **92**, 107401 (2004).
15. K. J. K. Koerkamp, S. Enoch, F. B. Segerink, N. F. van Hulst, and L. Kuipers, "Strong Influence of Hole Shape on Extraordinary Transmission through Periodic Arrays of Subwavelength Holes," *Phys. Rev. Lett.* **92**, 183901 (2004).
16. L. Collot, V. Lefevre-Seguín, M. Brune, J. Raimond, and S. Haroche, "Very high-Q whispering-gallery mode resonances observed on fused silica microspheres," *Europhys. Lett.* **23**, 327 (1993).
17. M.-H. Wu and G. M. Whitesides, "Fabrication of arrays of two-dimensional micropatterns using microspheres as lenses for projection photolithography," *Appl. Phys. Lett.* **78**, 2273 (2001).
18. D. Bäuerle, T. Gumpenberger, D. Brodoceanu, G. Langer, J. Kofler, J. Heitz, and K. Piglmayer, in *Laser Cleaning II*, edited by D.M. Kane (World Scientific, Singapore, 2005).
19. D. Bäuerle, G. Wysocki, L. Landström, J. Klimstein, K. Piglmayer, and J. Heitz, "Laser-induced single step micro/nanopatterning," *Proc. SPIE* **5063**, 8 (2003).
20. K. Piglmayer, R. Denk, and D. Bäuerle, "Laser-induced surface patterning by means of microspheres," *Appl. Phys. Lett.* **80**, 4693 (2002).
21. G. Wysocki, R. Denk, K. Piglmayer, N. Arnold, and D. Bäuerle, "Single-step fabrication of silicon-cone arrays," *Appl. Phys. Lett.* **82**, 692 (2003).
22. D. Bäuerle, K. Piglmayer, R. Denk, and N. Arnold, "Laser-Induced Surface Patterning by means of Microspheres," *Lambda Highlights* **60**, 1 (2002).
23. D. Bäuerle, *Laser Processing and Chemistry*, 3rd ed. (Springer Verlag, Berlin, 2000).
24. L. Landström, J. Klimstein, G. Schrems, K. Piglmayer, and D. Bäuerle, "Single-step patterning and the fabrication of contact masks by laser-induced forward transfer," *Appl. Phys. A* **78**, 537 (2004).
25. G. Langer, D. Brodoceanu, and D. Bäuerle, "Femtosecond laser fabrication of apertures on two-dimensional microlens arrays," *Appl. Phys. Lett.* **89**, 261104 (2006).
26. A. Pikulin, N. Bityurin, D. Brodoceanu, G. Langer, and D. Bäuerle, "Hexagonal structures on metal-coated two-dimensional microlens arrays," *Appl. Phys. Lett.* **91**, 191106 (2007).
27. L. Landström, D. Brodoceanu, N. Arnold, K. Piglmayer, and D. Bäuerle, "Photonic properties of silicon-coated colloidal monolayers," *Appl. Phys. A* **81**, 911 (2005).
28. L. Landström, N. Arnold, D. Brodoceanu, K. Piglmayer, and D. Bäuerle, "Photonic properties of silicon-coated monolayers of colloidal silica microspheres," *Appl. Phys. A* **83**, 271 (2006).
29. L. Landström, D. Brodoceanu, K. Piglmayer, and D. Bäuerle, "Extraordinary optical transmission through metal-coated colloidal monolayers," *Appl. Phys. A* **84**, 373 (2006).
30. R. Micheletto, H. Fukuda, and M. Ohtsu, "A simple method for the production of a two-dimensional, ordered array of small latex particles," *Langmuir* **11**, 3333 (1995).
31. S. G. Rodrigo, F. J. Garcia-Vidal, and L. Martin-Moreno, "Influence of material properties on extraordinary optical transmission through hole arrays," *Phys. Rev. B* **77**, 075401 (2008).
32. A. Krishnan, T. Thio, T. J. Kim, H. J. Lezec, T. W. Ebbesen, P. A. Wolff, J. Pendry, L. Martin-Moreno, and F. J. Garcia-Vidal, "Evanescence coupled resonance in surface plasmon enhanced transmission," *Opt. Commun.* **200**, 1-7 (2001).

1. Introduction

Extraordinary optical transmission (EOT) through thin metal films has attracted increasing interest in the last few years [1, 2]. EOT observed in symmetrically perforated thin metal films [3, 4, 5, 6], the squeezing of the optical near-field by plasmon coupling resulting in focusing light into very small volumes[7], and beaming of light via a single slit (or hole) in thin metal films surrounded by a grating like structure [8] are only a few of many interesting examples. A vast number of applications have been suggested and some are currently in use, e.g., wavelength tunable filters, sub-wavelength lithography, near-field microscopy, surface en-

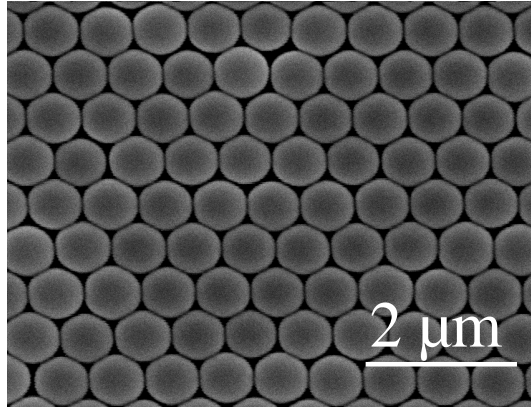


Fig. 1. Scanning electron microscope (SEM) picture of a Ni-coated monolayer of quartz (a-SiO₂) microspheres of diameter $d = 0.72 \mu\text{m}$. The support is a 1.0 mm thick a-SiO₂ platelet.

hanced Raman spectroscopy, etc.

Recent papers involve experiments and simulations of metal films and gratings of rather simple geometry[3, 5, 6, 9, 10, 11, 12, 13, 14, 15]. One drawback, considering applications, with these structures is that they are usually produced via focused ion beam material removal and/or complex, multi-step lithographic methods. In the present report we analyze metalized slabs of self-assembled arrays of microspheres, which show many similarities in transmission properties with those in perforated metal films, with the advantage of being easily deposited over relatively large areas. Moreover, the following metal deposition can be done by standard techniques.

Microspheres of different materials have been utilized in various fields of research in the past few years. Examples of applications are micro-resonators with high quality factors [16], in mask lithography [17], and also as lens arrays for different types of laser-induced micro- and nano-patterning of material surfaces. In case of laser-induced applications, close-packed two-dimensional (2D) lattices of usually transparent microspheres are used as a lens array allowing single step large area parallel processing[18, 19, 20, 21, 22]. Among those are patterns generated from metal-coated monolayers of microspheres by laser-induced forward transfer (LIFT)[23, 24, 25, 26].

Monolayers of close-packed arrays of microspheres behave like 2D photonic-crystal slabs (PCS) with photonic modes that may couple to the incident light. It has been shown that the strength of coupling and the position of the observed transmission dips could easily be altered by deposition of, e.g., amorphous Si onto the microsphere arrays [27, 28]. If the microsphere array is instead covered with a thin metal film, EOT through the slab has been observed[29].

In this paper we present new experimental results and analyze the transmission spectra with by finite difference time domain (FDTD) modeling. The good agreement between measured and modeled spectra allows further in-depth interpretation of the origin of the different features observed in the measured transmission spectra, highlighting the relevance of waveguide modes in the microsphere array on the EOT properties.

2. Methods

2.1. Experiment

Close-packed monolayers of amorphous silica ($a\text{-SiO}_2$) or polystyrene (PS) microspheres (diameters $d = 0.39, 0.78, 1.0, \text{ and } 1.42 \mu\text{m}$) were deposited on quartz supports (1 mm thick) using colloidal suspensions. The areas of close-packed monolayers were, typically, of the order of $\sim\text{cm}^2$. Because of certain size dispersion of the microspheres and the deposition technique employed [30], the monolayers exhibit a polycrystalline structure with a typical domain size of about 50-100 μm . The monolayers were covered with different metals (Ag, Au, Ni) and film thickness (30 - 300 nm) using standard evaporation techniques. A typical metal covered monolayer is shown in Figure 1.

Transmission experiments were performed at normal incidence on both bare PCSs and slabs covered with different metals (Ag, Au, Ni). The measurements were done in the far-field, in a configuration that only collected the zero-order transmission. The metal films cover approximately the upper half of single spheres, while the lower half remains uncoated. At the top of spheres the thickness of the coating is about equal to that measured with a nearby quartz crystal microbalance (QCM). Towards the equator, the film thickness slightly decreases. In the interstices between the spheres, the coating is placed on the quartz support. Within these areas, the film thickness measured by means of an atomic force microscope (AFM), is equal to that measured by QCM. Zero order transmission spectra within the region 300 - 2500 nm were recorded by means of an ultraviolet to near infrared spectrometer (Cary 500). Because of some size dispersion of the microspheres, the monolayers exhibit a polycrystalline structure with typical domain sizes of about 50-100 μm . Since aperture diameters of 1-3 mm were used for the transmission measurements, any polarization dependent effects could not be probed and non-polarized light was used.

2.2. FDTD Modeling

Simulations were performed by using the Finite Difference Time Domain (FDTD) method. A small grid size of 6 nm was used in all reported results. The dielectric constant of the different metals considered were taken from their bulk values, and approximated by a Drude-Lorentz functional form (the details can be found in Ref.[31]). Dielectric constants for the quartz support, and the silica and polystyrene microspheres were assumed wavelength independent and set to 1.52, 1.392 and 1.572, respectively. As the geometry of the metal layer is not precisely known, for simplicity the thickness of the metal film on the top of each sphere was assumed to be constant. In addition, slightly different thickness values than the experimentally observed have been used to commensurate to the mesh size. However, we expect that this simplification of the metal geometry will induce at most some small spectral displacements of the transmission resonances and of the average transmittance, but will otherwise have a negligible effect on the overall transmission properties of the system. In order to compare with the experimental transmittance, only transmission into the zeroth diffraction order was computed.

3. Results and discussion

Figure 2 compares measured and modeled spectra for silica sphere arrays covered with Ni, Ag and Au metals. Overall, the modeled spectra reproduce quite well the observed features with respect to both the absolute transmission values and peak positions. The main difference that can be observed is the additional peak at around 1300 nm in the calculated spectra. For the case of Ni, this peak seems to be hidden under the shoulder of the main peak. For Ag and Au it seems to be absent in the measured spectra. All peaks in the measured spectra are also slightly broader, likely because of the size-dispersion of the spheres and the polycrystalline structure

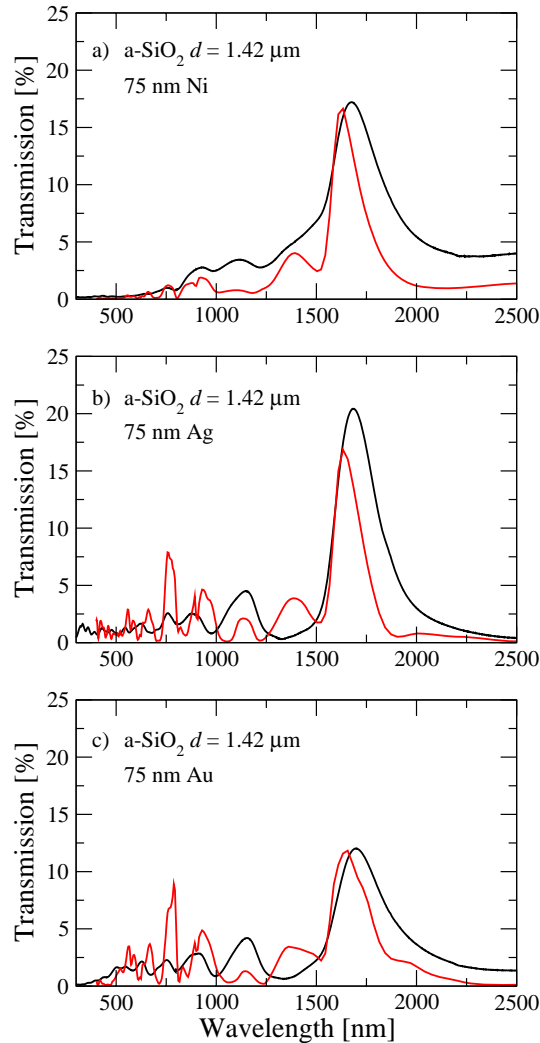


Fig. 2. Measured (black) and calculated (red) zero order transmission through metal coated MLs of a-SiO₂ microspheres ($d = 1.42 \mu\text{m}$).

of the array. Nevertheless, the overall good agreement suggests that this simple fabrication route leads to structures where disorder is small enough as not to spoil the optical transmission resonances expected in perfect arrays.

In the optical regime, the different behavior of the metals is notable. The peaks for Ni are less pronounced, while Ag and Au presents more detailed fine structure in both measured and modeled spectra. This effect is related to the difference in optical properties of these metals. Nickel is a less "ideal" metal with relatively high absorption in the wavelength region of interest, resulting in less pronounced features in both measured and modeled spectra. The calculated spectra for gold and silver have more defined (and stronger) peaks in comparison to the measured ones at shorter wavelengths. This may be due to the presence of disorder in the sample, where not all unit cells are strictly equal. Also, films deposited onto the microsphere arrays exhibit a poly/nano-crystalline structure, which may alter the optical properties of the metal

relative to bulk values used in the calculations. Both such alterations impair resonant behavior, being therefore more evident in Ag and Au than in Ni (where resonances are already hampered by intrinsic absorption of the metal).

The situation is different in the telecom regime (transmission peaks appearing around 1600 nm in Fig. 2). In this case, the transmission levels for all metals considered is similar, being even larger for Ni than for Au or Ag. Notice that, in this case, the full-width-at-half-maximum ($\Delta\lambda$) is very very similar for all three metals considered: 163 nm for Ni, 154 nm for Ag and 126 nm for Au. Given that the dielectric constant of Ni is very different from that of Ag and Au, this implies that the time that the electromagnetic field stays at the structure is limited by radiation, more than by absorption. This time can be estimated as $T = \lambda_{max}^2 / (c\Delta\lambda)$ and the distance that the EM field travels on the surface as $L_T = \lambda_{max}^2 / \Delta\lambda$, where λ_{max} is the spectral position of the transmission maximum and c the speed of light. From the simulation we can estimate $L_T = 16.2 \mu\text{m}$, $17.4 \mu\text{m}$ and $12.6 \mu\text{m}$ for Ni, Ag and Au, respectively. These values are smaller than, for instance, the propagation lengths of surface plasmon polaritons at $\lambda = 1600$ nm (which approximately are $25 \mu\text{m}$ for Ni, $360 \mu\text{m}$ for Ag and $360 \mu\text{m}$ for Au), which reinforces the hypothesis that radiation losses dominate over absorption. Notice also that the larger absorption in the case of Ni could be compensated by the larger skin depth (33 nm in Ni, 22 nm in Ag and 23 nm in Au for $\lambda \approx 1600$ nm), which implies both a larger direct transmission through the metal layer and a larger effective hole radius.

To further study the behavior of this composite structure and the validity of using the FDTD method, different parameters were investigated. Here, the refractive index of the spheres was changed by considering polystyrene microspheres. The sphere diameters (periodicity) was also altered, see Figure 3. As expected, by using monolayers of polystyrene spheres (with a higher refractive index than a-SiO₂) with different diameters, one finds that the main peak shifts with the periodicity of the array. Again, measured and modeled spectra show good agreement (Figure 3). We associate the higher values for the calculated peaks both to disorder in the actual sample and to the fact that absorption in the PS spheres was neglected in the calculations.

The main peak is further red-shifted relative to the diameter by about a factor of $1.3d$, whereas a factor of $1.2d$ was observed for the silica spheres (Figure 2). This is related to the higher refractive index of the polystyrene spheres relative to silica. The same effect is observed for PCS without metal, that is, a higher "effective" refractive index red-shifts the main minima (dip) in transmission [27, 28]. Additionally, the main dip in the dotted curves in Figure 3, that show the transmission of the bare MLs, and the main transmission peak of the metal coated arrays show a clear correlation. The main transmission peak is slightly red-shifted compared to the main dip. This behavior implies that the transmission is related to the supported modes of the bare (uncoated) 2D photonic crystal slab as suggested earlier [29]. The transmission spectra of the bare PCSs are also included in the graphs where once again can see the differences in the transmission curves. The modeled spectra show much narrower main dips than the measured ones, again pointing to the influence of absorption in the PS spheres, and also to size dispersion of spheres and grain boundaries within the monolayers. In any case, as can be seen in Figure 3, our fabrication method allows for simple scaling (positioning) of any transmission peak (or dip) of interest. It is also demonstrated in Figure 3c that the main peak can be easily shifted to the visible wavelength region. This could be interesting with possible application for these composite structures as, e.g., for the fabrication of relatively narrow band filters.

Importantly, the close spectral correspondence between transmission dips in the uncoated system and transmission peaks in the coated one is also present in the calculation, even more clearly so, as spectral features are narrower here than in the experiment.

The thickness of the metal deposit was also varied for both Ag and Au metals on silica spheres, see Figure 4. For both metals, the intensity of the main transmission peak decreases

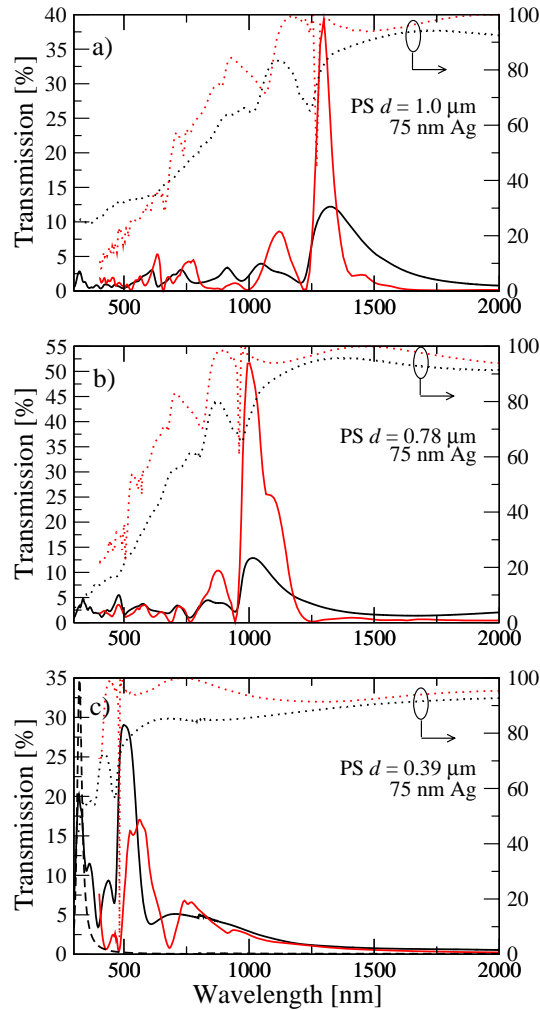


Fig. 3. Measured (black) and modeled (red) zero order transmission through monolayers of polystyrene spheres. Bare monolayer - dotted curves (right y-scales) and coated with 75 nm silver - full curves (left y-scales). a) $d = 1.0 \mu\text{m}$, b) $d = 0.78 \mu\text{m}$, c) $d = 0.39 \mu\text{m}$. The main peak (or dip) scales with the periodicity (d).

roughly exponentially. Notice that the measured transmission is higher for thicker deposits compared to modeled spectra, which we associate to the assumption of homogenous film thickness in the calculations. Again, quite large discrepancies can be observed between measured and calculated spectra in the short wavelength region. Also, the main peak red shifts as the thickness is increased. (More pronounced for the measured spectra.) Possibly, this can be related to coupling of the modes on the two interfaces; PCS/metal and metal/air. For films with thickness less than 50 nm, two peaks can be observed in the calculated spectra, whereas only one peak is observed for the thicker deposits, suggesting a coupling/decoupling behavior of the two modes as the thickness is increased.

The rest of the paper is devoted to ascertain which are the relevant mechanisms for the transmission resonances in this system. Notice that the composite slab is quite complex, and transmission resonances could be due to one or several factors, like: surface plasmons coupled either

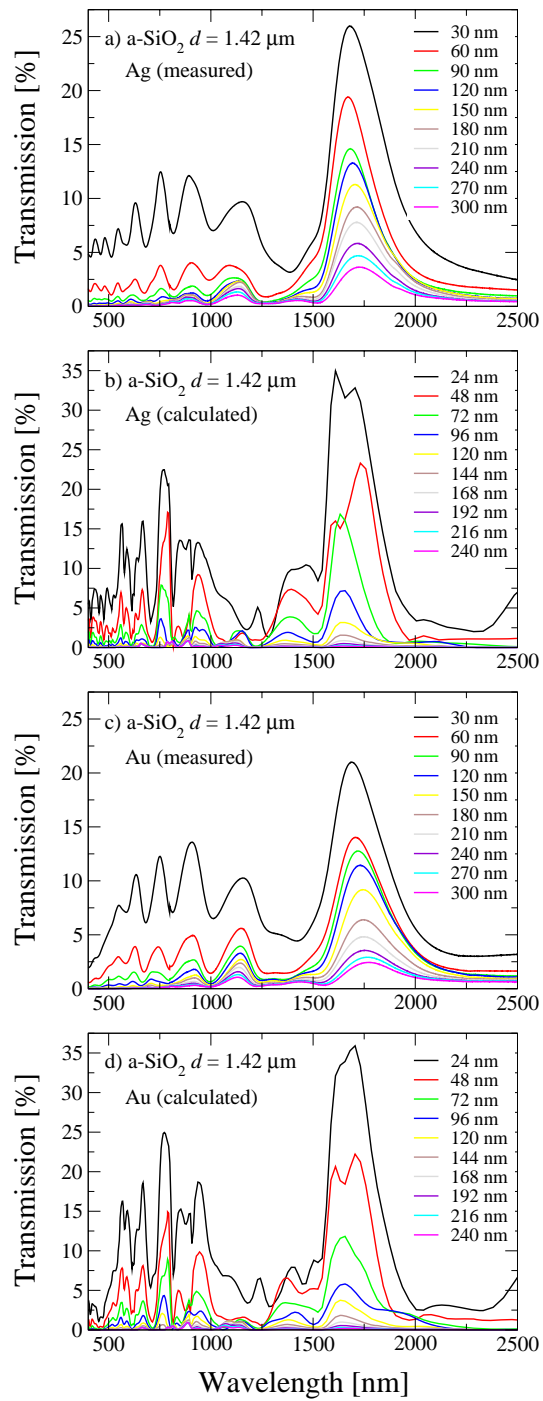


Fig. 4. Measured (a, c) and calculated (b, d) transmission spectra for different thicknesses of the metal deposit. Ag and Au were used on $d = 1.42 \mu\text{m}$ silica spheres.

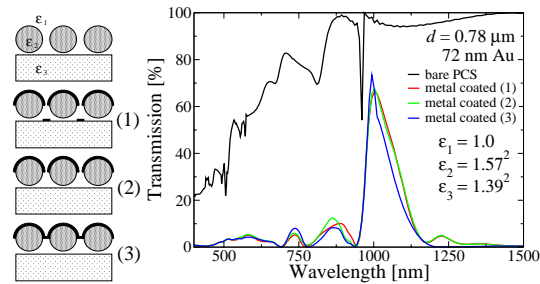


Fig. 5. Calculated transmission curves for bare PCS and with different metal coverage (1)-(3).

through the holes in the interstices or through the metal (if the metal film is optically thin), photonic crystal modes in the sphere layer (weakly or strongly coupled), Mie resonances of the spheres, particle plasmon modes of the triangular metal deposit on the quartz support, etc. The good agreement between measured and calculated spectra allows us to study of the relevance of these different mechanisms, through the modeling of similar but simpler systems.

To start with, two different but related structures were modeled: Metal coated sphere arrays without any metal on the support and sphere arrays fully covered with metal (and consequently no metal on support either). The calculated results are shown in Figure 5. Interestingly, the calculations reveal that the metal deposit on the support has negligible influence on the overall transmission and, more importantly, that the transmission spectra remains practically unaltered if the holey metal cap covering the spheres is replaced by a continuous metal cap. So, for this parameter range, the coupling across the metal film is mainly due to coupling through the metal, and not through the holes. This calculation also shows that there is no need for improvements in the fabrication process in order to get rid of the deposited metal on the substrate.

In order to investigate the importance of a PCS and its guided modes as support to the metal film, the spheres were simply removed in the model system by introducing a uniform refractive index below the corrugated metal film (both with and without holes). In this case, the transmission process can be explained by a resonant model involving surface plasmon excitations and tunneling through the corrugated thin metal film[5, 32]. The results are depicted in Figure 6. Remarkably, in the uniform dielectric case, absolute transmission values are much lower than those obtained for the sphere system. In addition, we have computed the transmission for a thin planar film with triangular holes (with the same size as those in the experiment) in graphene symmetry. Again transmission values are low when compared with those in the capped sphere system. These findings suggest that the presence of the photonic crystal layer is of great importance in the overall transmission mechanism. The close spectral correspondence between transmission peaks in the coated case and transmission dips in the uncoated one, already points to the possible relevance of guided modes in the photonic crystal. This relevance is corroborated by the computed electromagnetic field distributions (see Figure 7 for a representative case), which present strong field confinement at the location of the spheres.

It is interesting to highlight the differences on the transmittance between guided modes in a photonic crystal and guided modes in a uniform dielectric slab. The first difference is related to the "energetics". A first estimation of the spectral position at which EOT features appear can be obtained by computing the frequency of the surface mode involved, at a wavevector equal to the shortest reciprocal lattice vector (for the case of normal incidence considered here). Similarly, dips in the corrugated dielectric are expected to appear at the same condition, as Figure 3 shows. Let us start by considering the uniform dielectric slab. The point here is that the guided

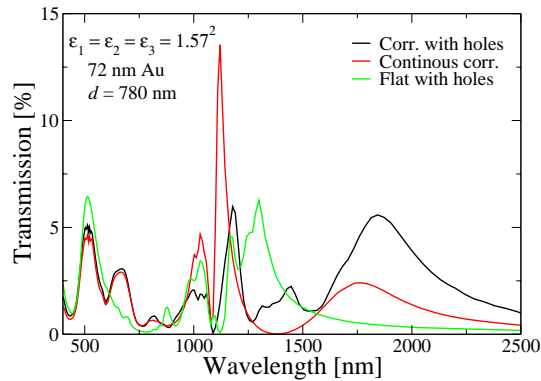


Fig. 6. Calculated transmission curves for corrugated (with and without holes) and planar metal film with holes in a graphene symmetry. All films were modeled in a homogeneous media. The metal considered is Au and the lattice parameter is $d = 780$ nm.

modes in a vacuum-metal-dielectric film-substrate (VMDS) waveguide are different from the ones in a vacuum-dielectric film-substrate (VDS) configuration, due to the large differences between the Fresnel coefficients for metal/dielectric and metal/air interfaces. Therefore, features in a corrugated dielectric and a corrugated metal, each of them placed on top of dielectric slab, should appear at different wavelengths. To illustrate this point, we have computed the wavelengths of the guided modes in both VMDS and VDS configurations, for the following parameters (motivated by the experimental setup): the dielectric film has a dielectric constant $\epsilon = 1.57^2$ and a thickness $t = 780$ nm. The substrate has a dielectric constant $\epsilon = 1.5^2$. The considered wavevector is $k = 2\pi/t$ (in a sphere array the inter-distance between spheres is equal to the dielectric film thickness). The metal thickness is 70 nm and its dielectric constant is taken as $\epsilon_{metal} = -50$ (approximately the value for Au at $\lambda \sim 1000$ nm). We obtain that the wavelengths of the guided modes are: 1176 nm for the VDS configuration and 1235 nm for the VMDS case. On the contrary, the dispersion relation of guided modes in the photonic crystal (composed by the two-dimensional arrays of dielectric spheres) is weakly affected by the presence of the metal film (calculations not presented here estimate that the difference between the wavelengths of the guided mode in the metal capped and un-capped configurations is of the order of 5 nm). This is so because, in this case, the z-component of the electric field (which is the relevant one for guided modes) is more concentrated close to the center of the spheres (see Fig. 7), so a smaller fraction of the field senses the different Fresnel coefficients alluded above.

The second difference is related to the coupling of the light, passing through the metal film in the presence of guided modes, to the different radiation orders. Guided modes in photonic crystals represent a weaker coupling to radiation modes than either guided modes in a dielectric or surface plasmons (again due to the previously cited concentration of the electric field in the photonic crystal guided modes). Notice that radiation damping impairs the resonant transmission process, so this feature of photonic crystal modes explains why the configuration of metal film on top of a photonic crystal is so efficient for EOT phenomena (see Fig. 5 and 6).

Finally, it must be noted that in the present report we have concentrated on the observed main transmission peak. However, the transmission behavior at shorter wavelengths also show a close correspondence between transmission dips in the uncoated system and transmission peaks in the coated one, again pointing to the relevance of guided modes. These modes could be due to either re-mappings (aided by a reciprocal lattice vector) of the fundamental guided mode or to higher order guided modes. No attempt has been made in this work to assign a definite origin

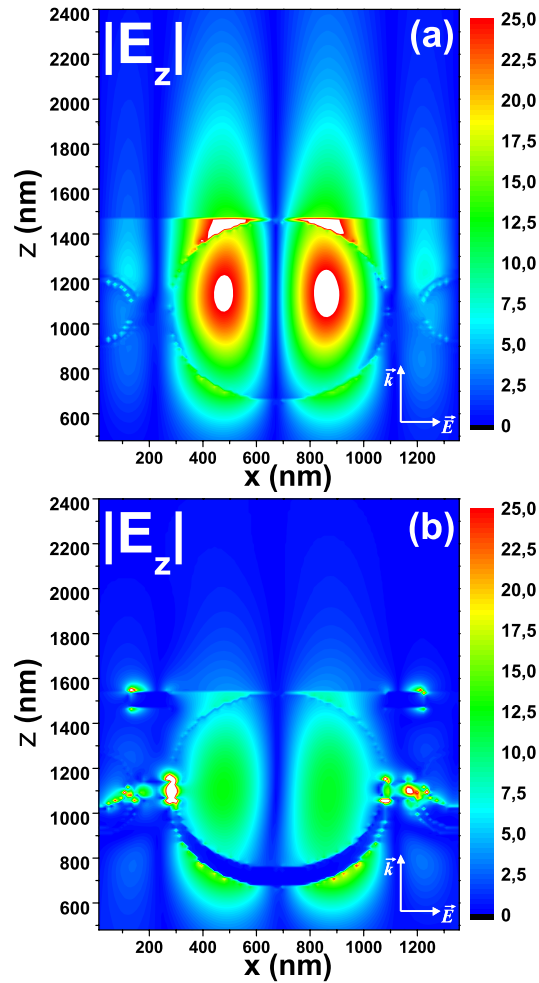


Fig. 7. Contour plots for the modulus of the z-component of the electric field across a plane passing through the center of the spheres. The system under study is the one considered in Figure 3 (b). Panel (a): uncoated case at the wavelength of the main transmission dip ($\lambda = 944$ nm). Panel (b): coated case at the main transmission maximum ($\lambda = 1002$ nm)

to these modes as they give rise to small transmission peaks.

4. Summary

In summary, high extraordinary optical transmission was observed in different microsphere based photonic crystal slabs covered with thin metal films. Measured spectra were compared with spectra calculated by FDTD calculation and the good agreement allowed modeling of slightly modified structures to get further information about possible transmission mechanisms. The calculations indicate that the guided modes in the PCS are mainly responsible to the relatively large transmission values observed (especially for the main peak). In contrast, the small holes in the thin metal film (at the interstices between three adjacent spheres) and metal deposit onto the support do not strongly influence the main transmission peak. The high transmission values, straight-forward fabrication and easy up-scaling of the metal covered slabs together

with simple peak positioning in a broad wavelength region (VIS/IR) make these structures a good candidate for different application purposes.

Acknowledgments

We thank financial support from the Austrian Research Fund FWF (Fonds zur Förderung der wissenschaftlichen Forschung) under contract no. L426-N14 and the Spanish MECD under contract MAT2005-06608-C02. One of us (L. L.) would like to thank the "Knut and Alice Wallenberg Foundation" for financial support.